UNIVERSITAT POLITÈCNICA DE CATALUNYA
BARCELONATECH

MSc. in Computational Mechanics
Industrial Training
Spring Semester 2017/2018

INTERNSHIP REPORT

Submitted By:
Luan Malikoski Vieira

Supervisor:
Prof. Josep Sarrate

External Supervisor:
Dr. David Modesto

September 3, 2018
Barcelona, Spain

Contents

Acknowledgments

I would like to express my gratitude to Professor Josep Sarrate who was the person that at the very first moment made this internship possible by contacting Dr. David Modesto.

I am very grateful to Dr. David Modesto, Dr. Josep de la Puente and Dr. Octavio Castillo for their disposal in accepting me as a intern in their study group in the BSC.

I can not forget to mention my special gratitude, again, to Dr. David Modesto and Dr. Octavio Castillo which dedicated their time to clarify all my doubts and taught me concepts that were valuable for this work and will be valuable for my prospective career.

Even though the internship had a relatively short duration I could learn really valuable concepts which opened my mind to one more perspective in this vast scientific world and for that I could not be more grateful.

Finally my gratitude for BSC and for all people I met there that made this short time an enjoyable one.

1 Introduction

This report will cover the activities carried out in the internship at Barcelona Supercomputing Center (BSC) in the period of 1^{st} of July to 1^{st} of September. The training took place at the Computer Applications in Science and Engineering (CASE) sector and was mainly focused on parametric solution of Controlled Source Electromagnetic (CSEM) problems using a priori model order reduction (MOR) technique named as Proper generalized Decomposition (PGD).

The specific focus was given for implementing a Total Field formulation of the electromagnetic source in a PGD framework with dipole frequency (ω) and source position (S_p) as basis of the parametric space. In this work the called Edge Finite Element (EFEM) technique is adopted for the spatial discretization of the governing equations. Thus, the two main tasks were performed during the internship:

- Preliminary studies on the existent EFEM prototype code for the approximated solution of CSEM problems.
- Implementation of a Total Field formulation of the electric field in a PGD algorithm.

1.1 Motivation

Reduced order models are very attractive tool from the scientific and engineering point of view, specially in studies where the approximated solution of a model is required for a wide range of parameters. In most cases, the direct multi parametric solution of those problems are even unfeasible given time and computational resources constrains. In such a cases the application of an ROM algorithm is an option to tackle the problem. In this work the Proper Generalized Decomposition (PGD) is applied in order to obtain a parametric solution of the Maxwell equations for CSEM applications.

In this panorama, two formulations of the electric field model are possible: Field Decomposition (FD) and Total Field (TF). The first formulation, which involves a smooth source term in governing equation, has the advantage of providing an accurate enough solution in which the mesh does not need to be adapted to the source. On the other hand, when we move to a PGD framework, from a computational point of view, this approach requires more memory and computations in order to pre-compute and assemble the matrices related with the source term, respectively. Thus, a trade-off exist when a Total Field formulation is used in a PGD approximation to overcome the FD approach limitations.

In this work, the implementation of the PGD algorithm with the TF formulation will be presented and this trade-off discussion will be initialized.

2 Preliminary studies on the EFEM code

This section is devoted to present the preliminary study of the spatial discretization technique applied to 3D Maxwell's equations. A prototype code on 3D Edge Finite Elements (EFEM) for CSEM problems was studied and some test cases were run. Two different formulation of the electric field were employed: Total field (TF) and Field Decomposition (FD). This preliminary study was necessary in order to get acquainted with all aspects of the problem to be solved, from the modelling to the EFEM approximation.

2.1 Model and weak formulation

The prototype EFEM code provides an approximated solution for Maxwell's equations in curl-curl formulation, in terms of Field Decomposition formulation (1,2) and Total Field formulation (3,4).

$$\nabla \times \nabla \times \mathbf{E_s} + i\mu\omega\sigma\mathbf{E_s} = -i\mu\omega(\sigma - \sigma_p)\mathbf{E_p} \quad in \quad \Omega \tag{1}$$

$$\mathbf{E_s} = 0 \quad on \quad \partial\Omega \tag{2}$$

$$\nabla \times \nabla \times \mathbf{E} + i\mu\omega\sigma\mathbf{E} = -i\mu\omega\mathbf{J_{sr}} \quad in \quad \Omega \tag{3}$$

$$\mathbf{E} = 0 \quad on \quad \partial\Omega \tag{4}$$

Where in (1), the solution is seek for the secondary field ($\mathbf{E_s}$) in terms of the known primary field ($\mathbf{E_p}$), with σ_p being the chosen uniform conductivity of the domain for the primary field. Then, the total field is recovered by $\mathbf{E} = \mathbf{E_s} + \mathbf{E_p}$.

In (3), the solution is already given in terms of the Total Field ($\mathbf{E}$), with $\mathbf{J_{sr}}$ being the point dipole source, mathematically described as pulse or Dirac delta.

The weak forms of equations (1) and (3), in the spatial coordinates $(x, y, z) \in \Omega$ is given respectively by the following:

$$(\nabla \times \delta\mathbf{E_s}, \nabla \times \mathbf{E_s})_\Omega + i\mu\sigma\omega(\delta\mathbf{E_s}, \mathbf{E_s})_\Omega = -i\mu(\sigma - \sigma_p)\omega(\delta\mathbf{E_s}, \mathbf{E_p})_\Omega \tag{5}$$

$$(\nabla \times \delta\mathbf{E}, \nabla \times \mathbf{E})_\Omega + i\mu\sigma\omega(\delta\mathbf{E}, \mathbf{E})_\Omega = -i\mu\omega(\delta\mathbf{E}, \mathbf{J_{sr}})_\Omega \tag{6}$$

Where $\delta\mathbf{u}$ is the test function of the approximated variable $\mathbf{u}$. And the L^2 product of the complex functions being defined as:

$$(\delta\mathbf{u}, \mathbf{u})_\Omega = \int_\Omega \delta\mathbf{u} \cdot \bar{\mathbf{u}} d\Omega$$

Where $\bar{\mathbf{u}}$ s the complex conjugate of $\mathbf{u}$.

2.2 Mesh study for Total Field and Field Decomposition formulations

The mesh size is changed in the .geo file which is ran in the *Gmsh* software. A mesh study was carried out using as parameter the variables **rg** and **rs**. The first is the number of elements per skin-depth (**sd**) distance in the global mesh such that $\mathbf{dg} = \mathbf{sd}/\mathbf{rs}$, where **dg** is the global element size. The second one defines the local element size (**ds**), at the receivers postion, such that $\mathbf{ds} = \mathbf{dg}/\mathbf{rs}$. A total of eight (8) meshes were tested for both Total Field (TF) and Field Decomposition (FD) formulations, as seen in table 1.

	M0	**M1**	**M2**	**M3**	**M4**	**M5**	**M6**	**M7**
rg	1	1	1	1	1.5	2	1.5	1.5
rs	3	6	12	18	6	6	12	18
Nº Elements [k]	10.4	11.6	19.1	38.0	36.8	80.0	64.1	128.5
Nº Nodes [k]	2.3	2.6	3.8	7.0	7.4	15.3	12.0	22.6
Nº Edges [k]	13.8	15.3	24.1	46.2	46.9	99.6	80.2	153.7

Table 1: Mesh parameters.

A L_2 like relative error norm ($E = \sqrt{\sum_i (x_i^{num} - x_i^{ref})^2} / \sqrt{(x_i^{ref})^2}$) of the numerical solution (x^{num}) with respect to a reference solution (x^{ref}) was evaluated for each mesh and formulation (FD or TF), results are shown in figure (1).

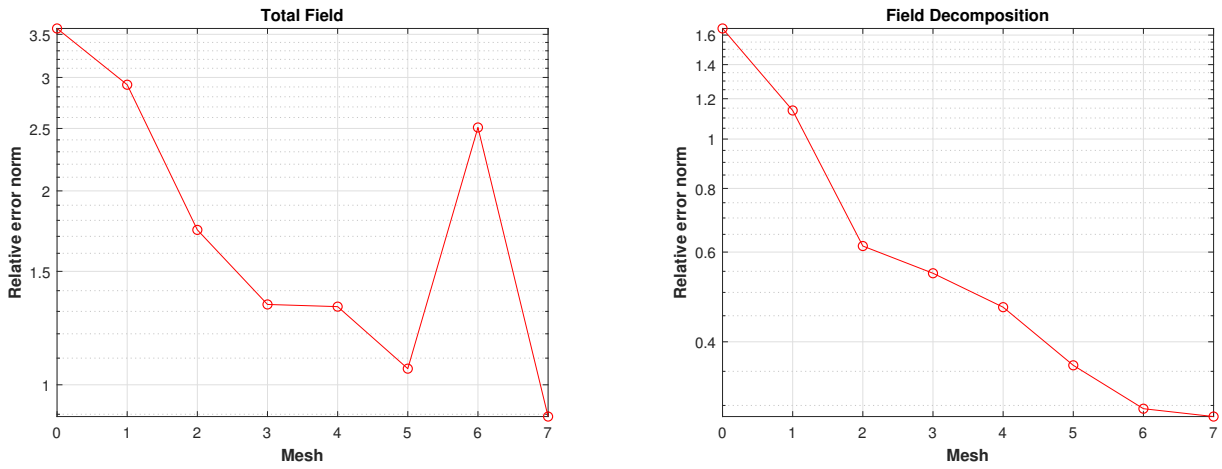

Figure 1: Relative error norm: (a) TF; (b) FD.

It can be observed in Figure (1) that as the mesh is refined, in general more accurate results are obtained for both formulations (TF and FD). It can be observed that a global refinement has a better effect on the accuracy, however the increment in edge numbers is higher than when considering a local refinement, as seen on table (1). A simple comparison between meshes M1, M3 and M5 illustrate this aspect.

For the Total field case, mesh M6 represents a high relative norm error, this is due to a punctual discrepancy in the solution with respect to the reference data. As it can be observed in figure (2) which shows the relative errors at each receiver position for the meshes M0, M5, M6 and M7. It also shows the higher accuracy of the FD formulation with respect to TF, presenting a uniform error over the receivers range while the TF formulation lacks accuracy near the center for most meshes cases.

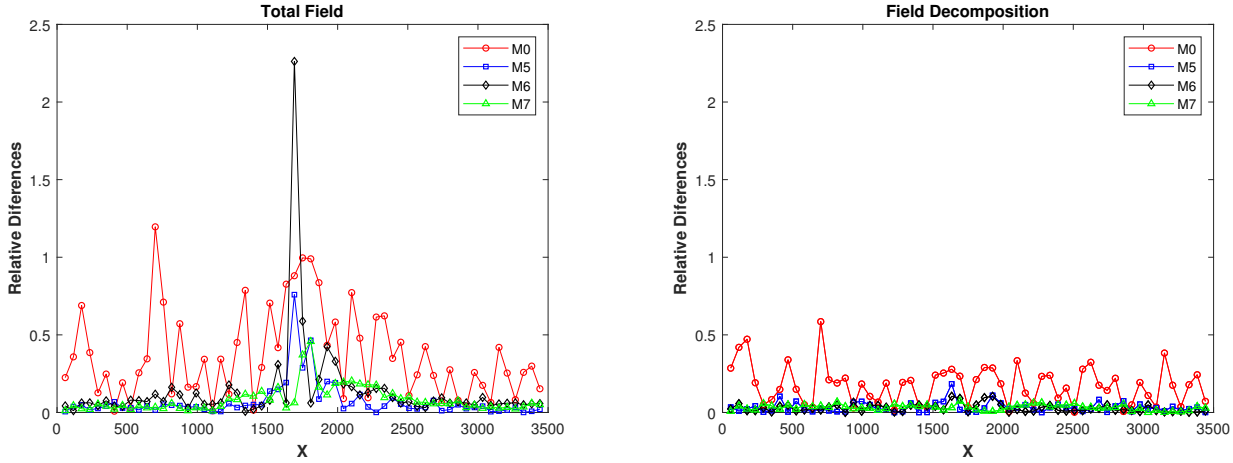

Figure 2: Relative differences at receivers M0, M5, M6 and M7 : (a) TF; (b) FD.

Results for the coarsest (M0) and finer mesh (M7) are shown below. The computed Electric field (E_x) at the receivers position is depicted in the plots. It can be observed that for the Total Field (TF) formulation a coarse mesh presents poor accuracy near center position and non-symmetric behavior. As the local refinement is increased this inaccuracy is reduced with respect to the reference solution.

For the Field Decomposition (FD) formulation a better accuracy near center is achieved with respect to the TF model.

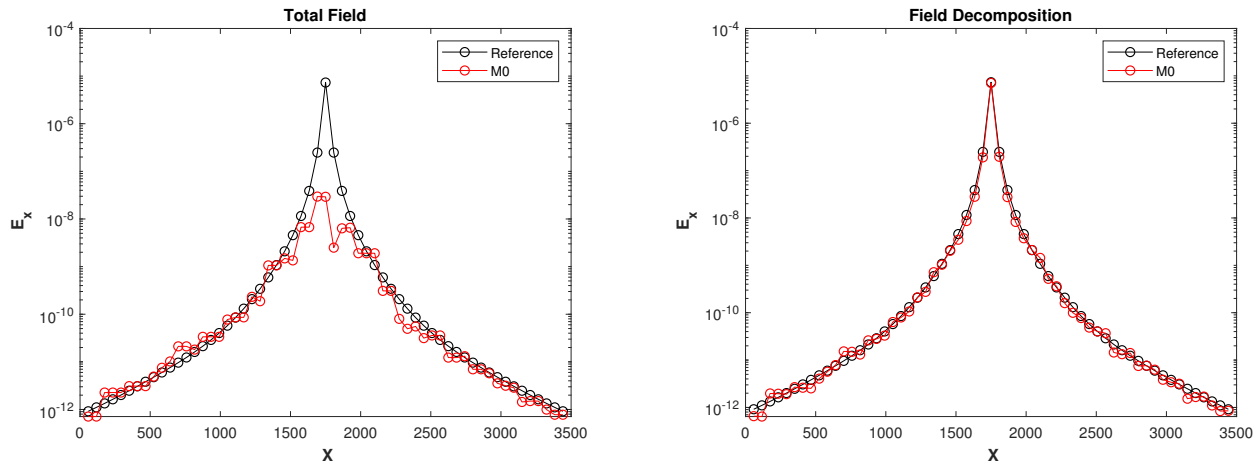

Figure 3: E_x at receivers - Mesh M0: (a) Total Field;(b) Field Decomposition

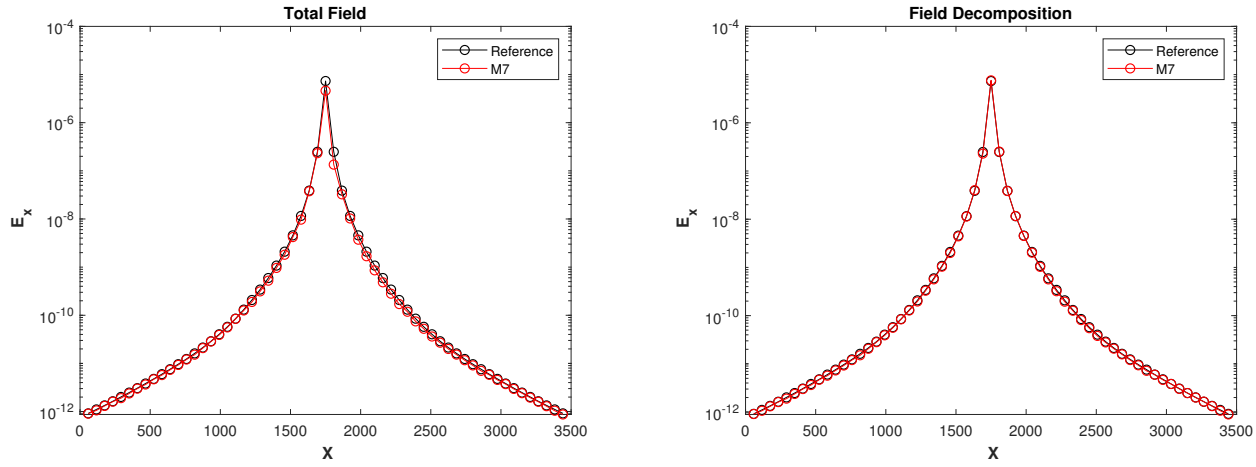

Figure 4: E_x at receivers - Mesh M7: (a) Total Field;(b) Field Decomposition

3 PGD Formulation and application

This section will present the PGD formulation for the studied CSME problem. A general formulation that applies for TF and FD approaches is presented. This formulation was already implemented for the Field Decomposition case, which was provided as a MatLab routine.

Next, particularities of the implementation of the FD and TF with respect to the source term are discussed. In the last subsection the performance of the implemented Total Field formulation in a PGD algorithm is evaluated.

3.1 General PGD Formulation

The PGD rationale is applied for parametrization of the eletric field in terms of the dipole source frequency (ω) and position (S_p). This gives rise to a five dimensional parametric space $(x, y, z, \omega, S_p) \in D$. The general weak form of the CSEM problem, from equations (5) and (6), in a five dimensional domain D can be written as:

$$(\nabla \times \delta\mathbf{E}, \nabla \times \mathbf{E})_D + j\mu\sigma(\omega\delta\mathbf{E}, \mathbf{E})_D = -j\mu(\omega\delta\mathbf{E}, \mathbf{S})_D \tag{7}$$

Where $(x, y, z) \in \Omega$, $(\omega, s_p) \in P$. For the total field case $\mathbf{S} := \mathbf{J_{sr}}$. While for the field decomposition case $\mathbf{E} := \mathbf{E_s}$ and $\mathbf{S} := \Delta\sigma\mathbf{E_p}$.

Now, the electric field is written in a separable form, break up into a vectorial ($\mathbf{F_1}$) and scalar function (F_2), as $\mathbf{E} = \sum_{m=1}^{n} \mathbf{F_1^m}(x, y)F_2^m(\omega, s_p)$, which can be expressed as:

$$\mathbf{E^n} = \mathbf{F_1^n}F_2^n + \mathbf{E^{n-1}} = \mathbf{F_1^n}F_2^n + \sum_{m=1}^{n-1} \mathbf{F_1}^m F_2^m$$

Now assuming a test function variation such that $\delta\mathbf{E} = \delta\mathbf{F_1}F_2 + \mathbf{F_1}\delta F_2$, we can obtain two weak forms to be solved in a iterative way for $\mathbf{F_1^n}$ and F_2^n when $\delta F_2 = 0$ and $\delta\mathbf{F_1} = 0$ respectively, as follows. The n superscript is dropped for the sake of readability.

$$(F_2, F_2)_P \cdot (\nabla \times \delta\mathbf{F_1}, \nabla \times \mathbf{F_1})_\Omega + j\mu\sigma(\omega F_2, F_2)_P \cdot (\delta\mathbf{F_1}, \mathbf{F_1})_\Omega = -j\mu(\omega\delta\mathbf{F_1}F_2, \mathbf{S})_D - \mathbb{L}_1^{n-1} \tag{8}$$

$$(\nabla \times \mathbf{F_1}, \nabla \times \mathbf{F_1})_\Omega \cdot (\delta F_2, F_2)_P + j\mu\sigma(\mathbf{F_1}, \mathbf{F_1})_\Omega \cdot (\omega\delta F_2, F_2)_P = -j\mu(\omega\delta F_2\mathbf{F_1}, \mathbf{S})_D - \mathbb{L}_2^{n-1} \tag{9}$$

With the vectors in the r.h.s. $\mathbb{L}_1^{n-1}$ and $\mathbb{L}_2^{n-1}$ accounting for the contribution of the known PGD terms in the expansion and can be written as:

$$\mathbb{L}_1^{n-1} = \sum_{m=1}^{n-1} (F_2^m, F_2^m)_P \cdot (\nabla \times \delta\mathbf{F_1}, \nabla \times \mathbf{F_1}^m)_\Omega + j\mu\sigma(\omega F_2^m, F_2^m)_P \cdot (\delta\mathbf{F_1}, \mathbf{F_1}^m)_\Omega$$

$$\mathbb{L}_2^{n-1} = \sum_{m=1}^{n-1} (\nabla \times \mathbf{F_1}^m, \nabla \times \mathbf{F_1}^m)_\Omega \cdot (\delta F_2, F_2^m)_P + j\mu\sigma(\mathbf{F_1}^m, \mathbf{F_1}^m)_\Omega \cdot (\omega\delta F_2, F_2^m)_P$$

After discretizing $\mathbf{F_1}$ and F_2 in its respective FEM formulation and evaluating the integrals of equations (8) and (9) we obtain the following set of algebraic equations to be solved in alternate direction algorithm for $\mathbf{F_1^n}$ and $\mathbf{F_2^n}$ respectively.

$$[(\mathbf{F_2}^T\mathbf{M_w}\mathbf{F_2})\mathbf{K_x} + (\mathbf{F_2}^T\mathbf{M_{wf}}\mathbf{F_2})\mathbf{M_{x\sigma}}]\mathbf{F_1^n} = \mathbf{f_1} - \sum_n [(\mathbf{F_2}^T\mathbf{M_w}\mathbf{F_2})\mathbf{K_x} + (\mathbf{F_2}^T\mathbf{M_{wf}}\mathbf{F_2})]\mathbf{F_1^{n-1}} \tag{10}$$

$$[(\mathbf{F_1}^T\mathbf{K_x}\mathbf{F_1})\mathbf{M_w} + (\mathbf{F_1}^T\mathbf{M_{x\sigma}}\mathbf{F_1})\mathbf{M_{wf}}]\mathbf{F_2^n} = \mathbf{f_2} - \sum_n [(\mathbf{F_1}^T\mathbf{K_x}\mathbf{F_1})\mathbf{M_w} + (\mathbf{F_1}^T\mathbf{M_{x\sigma}}\mathbf{F_1})\mathbf{M_{wf}}]\mathbf{F_2^{n-1}} \tag{11}$$

The vectors $\mathbf{f_1}$ and $\mathbf{f_2}$ in the r.h.s of both equations represents the source term contribution in the weak forms. Those terms are integrals in the 5D domain, as seen in the r.h.s of equations (8) and (9), as the source term $\mathbf{S}$ is not written in a separable form.

In order to avoid this full dimensional integration, the source term is made separable such that it can be approximated as:

$$\mathbf{S}(x, y, z, \omega, S_p) \approx \sum_{k=1}^{n_p} \mathbf{S_1}^k(x, y, z)S_2^k(\omega, S_p)$$

With n_p as the number of terms of the approximation. Considering this approximation, $\mathbf{f_1}$ and $\mathbf{f_2}$ becomes:

$$\mathbf{f_1} \approx -\sum_{k=1}^{n_p} j\mu(\omega F_2, S_2^k)_P \cdot (\delta\mathbf{F_1}, \mathbf{S_1}^k)_\Omega \tag{12}$$

$$\mathbf{f_2} \approx -\sum_{k=1}^{n_p} j\mu(\mathbf{F_1}, \mathbf{S_1}^k)_\Omega \cdot (\omega\delta F_2, S_2^k)_P \tag{13}$$

3.2 Source term contribution - Total Field and Field Decomposition

The separable form of $\mathbf{S}$, mentioned in the previous section, is found by means of the Singular Value Decomposition (SVD) of the matrix form of the source term, when it is evaluated in all 5D domain points. Such that it can be written as $\mathbf{S} = \mathbf{U}\mathbf{\Sigma}\mathbf{V}^T$. After, $\mathbf{S}$ can be approximated by the first k relevant components of the decomposition in order to reduce physical memory consumption and computation time.

In this work, from the algorithmic point of view, the SVD is performed in the elemental $\mathbf{S}^e$ matrix. For the Field Decomposition (FD) case, the source term ($\mathbf{S} = \Delta\sigma\mathbf{E_p}$) is a smooth function of x, y, z, ω and S_p. Thus, the integrals in Ω, in equations (12) and(13), are evaluated at all spatial Gauss points. From the elemental point of view, $\mathbf{S^e}$ will have the dimensions of $3n_g \times n_\omega n_{sp}$. With n_g, n_ω and n_{sp} being the number of Gauss points, number of points in ω direction and number of points in S_p direction respectively.

For the Total Field (TF) case, the source term can be written as $\mathbf{S} = IdS\delta(\mathbf{x} - S_p)\hat{\mathbf{e}}$. With I and dS being the dipole current and the dipole length respectively. The vector $\hat{\mathbf{e}}$ is the unitary dipole direction vector. Here the relation between the source and the frequency is taken as constant, equal to one.

The sampling property of the Dirac delta can be exploited within each element and the integrals in Ω can be evaluated only in the source location. This leads to a matrix $\mathbf{S^e}$ with dimensions $3 \times n_\omega n_{sp}$, as no Gauss points are required, only the source position (x, y, z).

With this in mind, equations (12) and (13) can be written as a elemental assembling with $\delta\mathbf{F_1}$ and $\mathbf{F_1}$ being evaluated at the elemental source position S_p^e, as follows.

$$\mathbf{f_1} \approx -\mathbf{A}_{e=1}^{n_e} \quad j\mu IdS(\omega F_2, 1)_P \delta\mathbf{F_1}(S_p^e) \cdot \hat{\mathbf{e}} \tag{14}$$

$$\mathbf{f_2} \approx -\mathbf{A}_{i=1}^{n_e} \quad j\mu IdS\mathbf{F_1}(S_p^e) \cdot \hat{\mathbf{e}}(\omega\delta F_2, 1)_P \tag{15}$$

Where n_e is the number of elements in the spatial mesh and S_p^e is a source position in the parametric set $\mathbf{S_p} = (S_{p1}, S_{p2}....S_{pn_{sp}})$ with location matching the element e. If there is no source position in the set matching the location of the element e, $\mathbf{f_1^e}$ and $\mathbf{f_2^e}$ will be zero. This comes to the fact that the Dirac delta function is only non-zero with $\mathbf{x} = S_p$, thus the only elements with a nonzero $\mathbf{f_1^e}$ and $\mathbf{f_2^e}$ will be those whose its location matches a source position in the parametric set $\mathbf{S_p} = (S_{p1}, S_{p2}....S_{pn_{sp}})$.

The smaller size of the elemental source matrices $\mathbf{S}^e$ for the TF formulation ($3 \times n_\omega n_{sp}$ against $3n_g \times n_\omega n_{sp}$) leads to a lower memory requirement in comparison with the FD formulations, once those matrices are pre-computed. Apart from that, the number of matrices to be pre-computed in the TF formulation is equal to n_{s_p} (10^1 to 10^3 usually) as the contribution is zero for elements not matching any source position. This also implies that inside the while loop of the PGD greedy algorithm, the assembly can only be made on those source elements, which means n_{s_p} assembling, providing an huge reduction in computation cost per loop.

While for the FD formulation this number is equal to the number of elements in the spatial mesh (10^5 to 10^6 usually). It also noteworthy to mention the high sparsity of the $\mathbf{S^e}$ matrix for the TF formulation while for the FD formulation the matrix is almost always full.

In the MatLab routine, the elemental source contribution of the n_e elements, for the FD formulation, or the contribution of the n_{sp} elements for the TF formulation are stored in two cell array entities, named here as $\mathbf{M_1}$ and $\mathbf{M_2}$.

In table 2 the memory required to keep the elemental source contribution in the RAM for both Total Field (TF) and Field Decomposition (FD) cases are compared. To illustrate, the spatial mesh M3 and a 81 parametric nodes mesh is chosen.

Formulation	**FD**		**TF**	
Cell Array	**M1**	**M2**	**M1**	**M2**
Size [Bytes]	6.97×10^7	1.19×10^9	2.30×10^3	1.85×10^4
Total Size[Bytes]	1.26×10^9		2.08×10^4	

Table 2: RAM memory cost for the pre computation of elemental source contribution.

From an algorithmic point of view, each component of the cell array $\mathbf{M_1}$ is $\mathbf{U}^e$ and each component of the cell array $\mathbf{M_2}$ is $(\mathbf{V\Sigma^T})^e$. Both togeter form the elemental SVD of the source matrix $\mathbf{S}^e$ written as $\mathbf{S}^e = \mathbf{U}^e(\mathbf{\Sigma V}^T)^e$.

For the FD case, all $3 \times n_g$ SVD terms were considered. If k terms are considered for each elemental $\mathbf{S}^e$ based on a chose tolerance, the values in (2) are reduced. For example, using a tolerance of 1×10^{-8} the size of $\mathbf{M_1}$ and $\mathbf{M_2}$ becomes 3.44×10^7 and 5.30×10^8 respectively, which is still much higher than the sizes obtained for the TF formulation.

3.3 Performance of the PGD with Total Field formulation

The performance of the PGD application with a Total Field formulation (TF) with respect to a Field Decomposition (FD) counterpart is evaluated is this subsection. For this, the spatial mesh 3 (M3), described in table (1), is chosen for all tests. The parametric space $(\omega, S_p) \in P$ is discretized with a 81 nodes uniform mesh ($n_\omega = n_{sp} = 9$) for all tests. The range of the parametric variables are $\omega* = [0.5, 2.0]$ Hz and $S_p = [50, 3450]$ m.

In Figure 5 it is presented the last term contribution of the PGD expansion, chosen here a an error indicator, as a function of the number of PGD terms for both FD and TF.

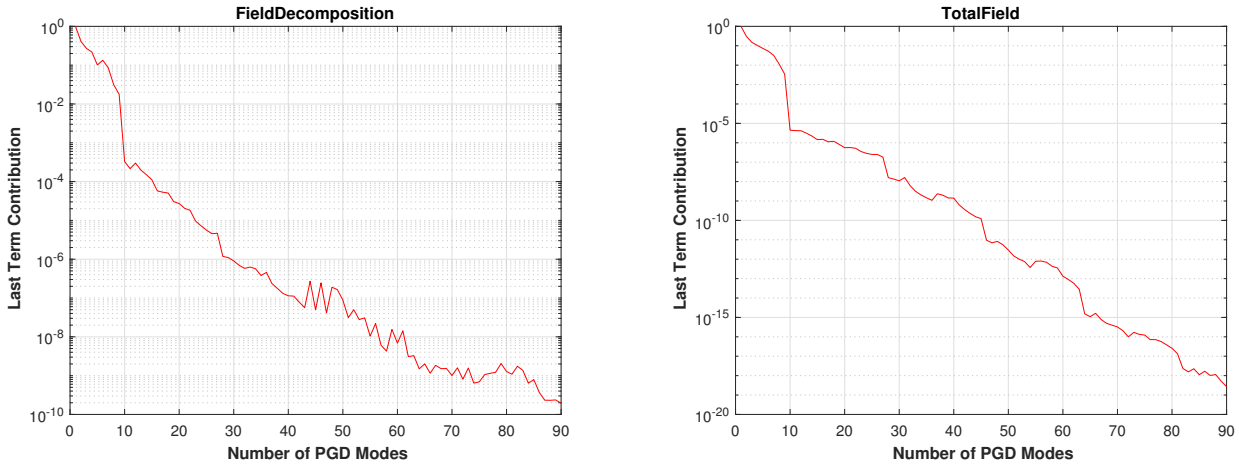

Figure 5: Last PGD term contribution:(a) Field Decomposition;(b) Total Field.

As observed in Figure 5, the last term contribution of the PGD approximation reduces faster for the TF formulation in comparison with the FD one as more terms are added to the PGD expansion. This is explained by the fact that the source term ($\mathbf{S}$) in the TF case has an SVD decomposition with less singular values (SVD modes) than the SVD decomposition of the source term for the FD formulation, as also discussed in the previous section. Thus, naturally it will be required more PGD modes to approximate the solution for the FD formulation, as the r.h.s. of its weak form is a term composed by more modes, or more relevant information.

It is also noticed that that after 9 PGD terms, both FD and TF present an drop in the error. This is related to the fact that the source position (S_p) is discretized with 9 nodes ($n_{sp} = 9$),thus an

better representation of this term is reached with nine or more modes.

In Figure 6, the L_2 norm error estimator is employed to evaluate the error of the PGD approximation with respect to the EFEM solution for different dipole frequencies (ω). The source position is kept fixed at $x = 1750$ m. As we can see for both FD and TF formulations the error decreases when the frequency increases.

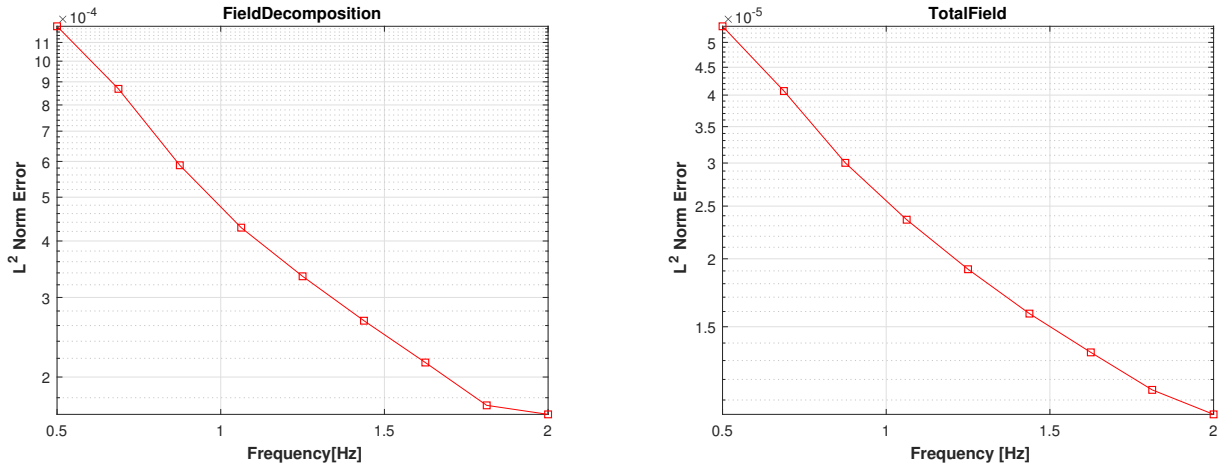

Figure 6: L^2 norm error with respect to frequency $\omega*$ - 90 PGD modes:(a) Field Decomposition;(b) Total Field.

In Figure 7, the L_2 norm error estimator is employed to evaluate the error of the PGD approximation with respect to the EFEM solution for different source positions S_p. The dipole frequency is kept constant as $\omega* = 2$ Hz. As we can see for both FD and TF formulations the error increases when the source position is near the boundary of the domain.

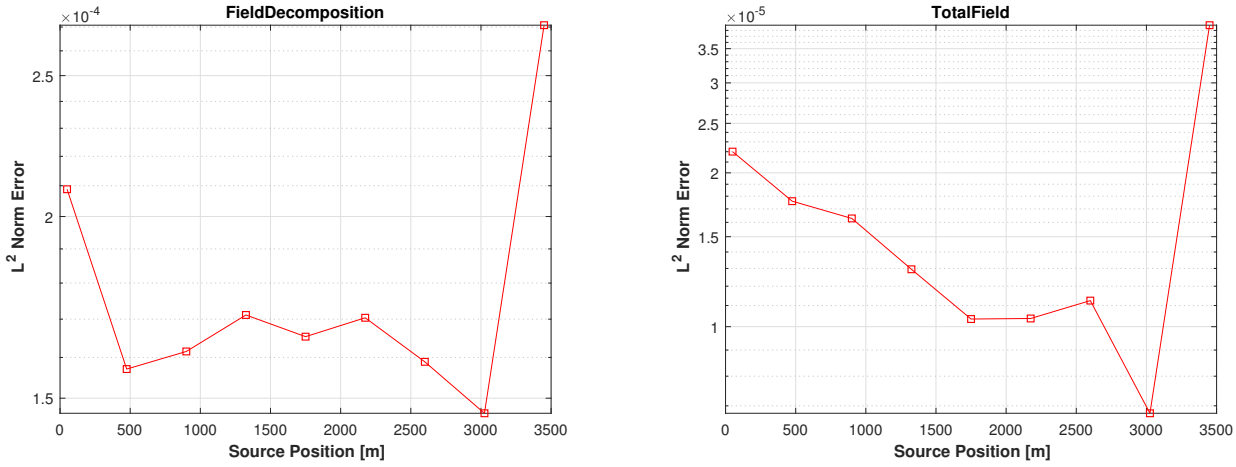

Figure 7: L^2 norm error with respect to source position S_p - 90 PGD modes:(a) Field Decomposition;(b) Total Field.

From both figures 6 and 7, it can be observed the the errors related with the FD formulation are one order of magnitude higher than the errors for the TF formulation. This is a natural result of what was explained before, in the sense that 90 PGD modes provides less accuracy for the FD formulation than for the TF formulation with respect to their respective EFEM solutions. Although, it is important to mention that even though the L^2 error norms for the FD formulation are higher,

it does not mean that the approximation with respect to a exact reference is less accurate than the same approximation for a TF formulations. This comes to the fact that the EFEM solution with a FD formulation is more accurate then a EFEM solution with TF formulation considering the same spatial mesh, as shown in section 2.2.

Finally, the comparison between EFEM and PGD approximation with the TF formulation are shown. In Figure 8 (a) it shows both approximations for 3 different dipole frequencies $\omega* = \{0.50 \quad 1.25 \quad 2.00\}$ Hz and source position fixed at $x = 1750$ m. Both approximations for 3 different source positions $S_p = \{900 \quad 1750 \quad 2600\}$ m and a constant frequency $\omega* = 2$ Hz are shown in Figure 8 (b).

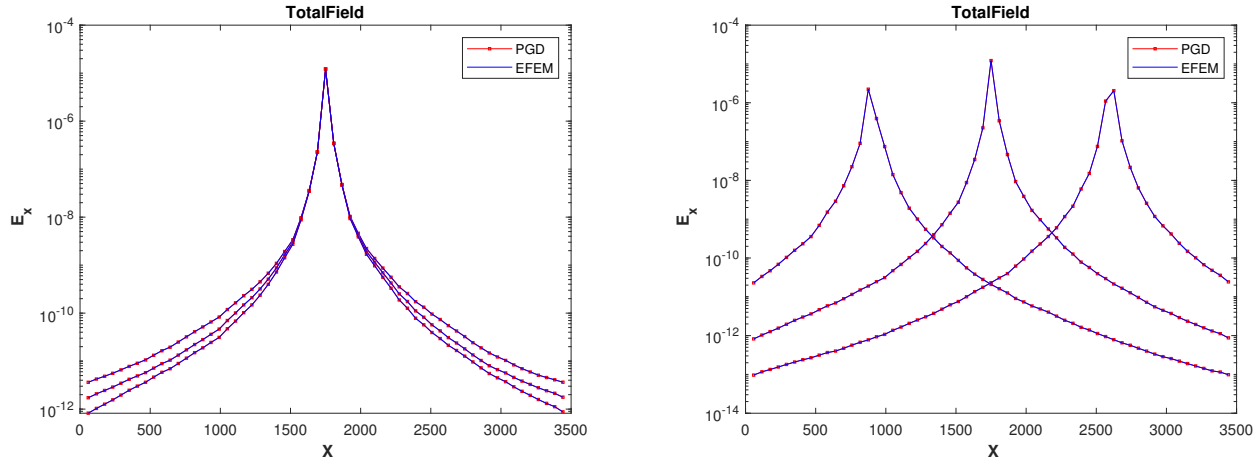

Figure 8: PGD solution with Total Field formulation compared with the EFEM solution - 90 PGD modes: (a) Variation in $\omega*$; (b) Variation in S_p

From both figures it can be observed that the proposed PGD approximation with a Total Field formulation provides same results as the EFEM approximation with the order of accuracy presented in figures 6 (b) and 7 (b).

4 Concluding remarks

The PGD approximation using a Total Field formulation for the electric field proved to be a fair option when dealing with problems presenting a considerable spatial and parametric size. This is because this approach proved to countermeasure the main drawback of a Field Decomposition based formulation, which is the high quantity of required memory RAM to dynamically allocate the matrices that arises from the source term. A simple test case presented in section 3.2, table 2, showed that the memory cost reduced from 1.26GB to only 20.80kB.

Apart from that, given the peculiarities of the Total Field formulation, a lower number of computation is required when assembling the elemental source term contribution inside the PGD loop.

Besides those advantages, the EFEM approximation using Total Field formulation is too much sensible with respect to the mesh, thus in some cases the lack of accuracy with respect to the Field Decomposition formulation is prohibitive, as shown in section 2.2. Said that, a fine enough mesh to ensure the desired accuracy of the EFEM approximation has always more degrees of freedom for a TF formulation than for a FD one.